© 2017. Published by The Company of Biologists Ltd | Development (2017) 144, 531 doi:10.1242/dev.148569

CORRECTION

Correction: Vegfc acts through ERK to induce sprouting and differentiation of trunk lymphatic progenitors

Masahiro Shin, Ira Male, Timothy J. Beane, Jacques A. Villefranc, Fatma O. Kok, Lihua J. Zhu and Nathan D. Lawson

There was an error published in Development **143**, 3785-3795.

In the Materials and Methods section we provided an incorrect serine residue number for the *map2k2b* mutation. The corrected section of text is as follows:

An activated myc-tagged form of MEK was generated from zebrafish *map2k2b* by mutating serines 221 and 225 to aspartic acid (Schramek et al., 1997) by PCR, followed by BP cloning to generate pME-*myc*-act-*map2k2b*.

In addition, we have since verified that the pME-*myc*-act-*map2k2b* plasmid used in the original studies and submitted to Addgene contains the correct sequence. This plasmid contains several nucleotide changes in comparison to the GenBank reference sequence (accession number: NM_001128281). However, all of these changes have been noted in a previous annotation of single nucleotide polymorphisms in the zebrafish and are naturally occurring variants (Butler et al., 2015).

We apologize for any confusion that this may have caused and we thank the researchers who discovered the error for bringing it to our attention.

Reference

Butler, M. G., Iben, J. R., Marsden, K. C., Epstein, J. A., Granato, M. and Weinstein, B. M. (2015). SNPfisher: tools for probing genetic variation in laboratory-reared zebrafish. *Development* **142**, 1542-1552.

© 2016. Published by The Company of Biologists Ltd | Development (2016) 143, 3785-3795 doi:10.1242/dev.137901

RESEARCH ARTICLE

Vegfc acts through ERK to induce sprouting and differentiation of trunk lymphatic progenitors

Masahiro Shin, Ira Male*, Timothy J. Beane, Jacques A. Villefranc‡, Fatma O. Kok, Lihua J. Zhu and Nathan D. Lawson§

ABSTRACT

Vascular endothelial growth factor C (Vegfc) activates its receptor, Flt4, to induce lymphatic development. However, the signals that act downstream of Flt4 in this context *in vivo* remain unclear. To understand Flt4 signaling better, we generated zebrafish bearing a deletion in the Flt4 cytoplasmic domain that eliminates tyrosines Y1226 and 1227. Embryos bearing this deletion failed to initiate sprouting or differentiation of trunk lymphatic vessels and did not form a thoracic duct. Deletion of Y1226/7 prevented ERK phosphorylation in lymphatic progenitors, and ERK inhibition blocked trunk lymphatic sprouting and differentiation. Conversely, endothelial autonomous ERK activation rescued lymphatic sprouting and differentiation in *flt4* mutants. Interestingly, embryos bearing the Y1226/7 deletion formed a functional facial lymphatic network enabling them to develop normally to adulthood. By contrast, *flt4* null larvae displayed hypoplastic facial lymphatics and severe lymphedema. Thus, facial lymphatic vessels appear to be the first functional lymphatic network in the zebrafish, whereas the thoracic duct is initially dispensable for lymphatic function. Moreover, distinct signaling pathways downstream of Flt4 govern lymphatic morphogenesis and differentiation in different anatomical locations.

KEY WORDS: Flt4, TALEN, Vegfc, Lymphatic, Zebrafish

INTRODUCTION

The lymphatic system comprises a series of blind-ended vessels that are connected to the circulatory system and play a central role in fluid homeostasis (Alitalo, 2011). Lymphatic vessels are also an important conduit for the immune system and facilitate lipid absorption in the digestive system. Among the important regulators of lymphatic vessel growth and maintenance are vascular endothelial growth factor c (Vegfc) and its receptor tyrosine kinase, Flt4 (also known as vascular endothelial growth factor receptor-3, Vegfr-3; Bahram and Claesson-Welsh, 2010). Flt4 is expressed specifically and dynamically on endothelial cells in the blood vascular and lymphatic systems. In both mouse and zebrafish embryos, *flt4* is expressed in actively sprouting endothelial cells, as well as endothelial cells lining large caliber veins and lymphatic vessels (Kaipainen et al., 1995; Siekmann and Lawson, 2007; Tammela et al., 2008; Thompson et al., 1998). Loss or reduction of *flt4* or *vegfc* leads to severe defects in lymphatic development in zebrafish and mouse (Hogan et al., 2009b; Karkkainen et al., 2004; Kuchler et al., 2006; Villefranc et al., 2013; Yaniv et al., 2006). In both cases, initial sprouting of lymphatic progenitors from large veins is blocked. Importantly, mutations in human *FLT4* or *VEGFC* are associated with congenital forms of lymphedema that are characterized by lymphatic hypoplasia (Gordon et al., 2013; Karkkainen et al., 2000). Thus, Vegfc signaling through Flt4 is essential for lymphatic development and this pathway is conserved in vertebrates.

Despite our knowledge of lymphatic vessel morphogenesis, less is known about what acts downstream of Flt4 *in vivo* to drive this process. In cell culture, common downstream effectors of receptor tyrosine kinases (RTKs), such as the serine/threonine kinases ERK (also known as MAP kinase) and AKT, can be activated in response to Flt4 dimerization (Deng et al., 2013; Makinen et al., 2001; Pajusola et al., 1994; Salameh et al., 2005; Wang et al., 2010). Moreover, specific tyrosine residues in the human FLT4 cytoplasmic domain have been implicated in the activation of distinct downstream targets and cellular outputs (Salameh et al., 2005). For example, Y1063 binds the adaptor molecule CRK and is required for activation of Jun N-terminal kinase (JNK; MAPK8), which facilitates endothelial cell survival. Similarly, Y1230 and Y1231 associate with the Grb2 adaptor to activate AKT and ERK, which promotes endothelial sprouting and proliferation (Salameh et al., 2005). Thus, FLT4 dimerization activates distinct downstream kinases to elicit different cellular outputs. However, the *in vivo* relevance of these studies is unclear and what acts downstream of Flt4 during lymphatic development is not well known.

An elegant approach to dissect RTK outputs *in vivo* is through the generation of animals bearing targeted mutations in residues within the cytoplasmic domain (Klinghoffer et al., 2002; Tallquist et al., 2000). This approach has been successful in implicating downstream effectors of vascular endothelial growth factor receptor-2 (Vegfr-2; also known as Kdr), a receptor for Vegfa that is similar to Flt4 and is essential for vascular development and angiogenesis (Koch et al., 2011). Mice bearing a point mutation in Vegfr-2 Y1173, which is essential for activating phospholipase c gamma 1 (Plcg1; Takahashi et al., 2001), exhibit defects similar to Vegfr2-null embryos (Sakurai et al., 2005). Zebrafish embryos mutant for *plcg1* also recapitulate loss-of-Vegfa phenotypes, underscoring the conserved nature of downstream Vegfa signaling components *in vivo* (Covassin et al., 2009, 2006; Lawson et al., 2003). Interestingly, loss of *plcg1* specifically affects artery development in the zebrafish, but lymphatic morphogenesis is normal (Lawson et al., 2003; Yaniv et al., 2006). This observation indicates that Plcg1, a presumed general RTK effector molecule, is selectively required for Vegfr-2, but not Flt4 signaling at this stage of development. Thus, there are clearly distinct downstream

Department of Molecular, Cell, and Cancer Biology, University of Massachusetts Medical School, 364 Plantation Street, Worcester, MA 01605, USA. *Present address: Department of Biology, University of Massachusetts, Amherst, MA 01003, USA. ‡Present address: Department of Surgery, Weill Cornell Medical College, New York, NY 10065, USA.

§Author for correspondence (nathan.lawson@umassmed.edu)

N.D.L., 0000-0001-7788-9619

Received 21 March 2016; Accepted 25 August 2016

Development (2016) 143, 3785-3795 doi:10.1242/dev.137901

signaling molecules activated by Vegfa and Vegfc in the different contexts of vascular and lymphatic development. However, targeted strategies to identify downstream Flt4 effectors *in vivo* have been limited.

The zebrafish is an ideal model in which to study lymphatic development (Kim and Jin, 2014). The external development and transparency of the zebrafish embryo permits direct visualization of lymphatic morphogenesis and forward genetic screens have yielded mutants affecting lymphatic development (Hogan et al., 2009a,b; Villefranc et al., 2013). In addition, the recent advent of programmable site-specific nucleases has enabled targeted deletions to be easily introduced into the zebrafish genome (Blackburn et al., 2013). In this study, we used transcription activator-like effector nucleases (TALENs; Christian et al., 2010) to generate embryos bearing targeted in-frame deletions in *flt4* to define downstream pathways important for lymphatic development. By comparing zebrafish embryos bearing a deletion that eliminates tyrosines 1226 and 1227 in the Flt4 cytoplasmic domain with embryos bearing a null *flt4* allele and with a *vegfc* mutant, we find that there are distinct requirements for signaling during facial and trunk lymphatic development. In particular, ERK is an essential effector that drives sprouting and differentiation of trunk lymphatic progenitors downstream of Vegfc. Moreover, phenotypic analysis of *flt4* alleles suggests that the facial lymphatic system is the first functional lymphatic network, whereas the thoracic duct is largely dispensable during zebrafish larval stages.

RESULTS

Generation of *flt4* mutant zebrafish lacking Y1226/7

To define signaling molecules that act downstream of Flt4 during early lymphatic development, we applied TALENs to generate targeted deletions in the zebrafish *flt4* gene. In this study we focused on Y1226 and Y1227 (Y1226/7), which are homologous to Y1230 and Y1231 (Y1230/1) in human FLT4 (Fig. 1A) where they are important for ERK and AKT activation in cell culture studies (Salameh et al., 2005). Unfortunately, we failed to identify active TALENs that could introduce lesions directly at Y1226/7 (data not shown). Therefore, we used two pairs of TALENs flanking the genomic sequence encoding Y1226/7 to generate zebrafish in which exons 27 and 28 were directly fused. We identified a founder fish bearing a lesion that results in a 23 amino acid in-frame deletion and eliminates Y1226/7 in the Flt4 cytoplasmic domain (Fig. 1A-C). The official allele designation for this allele is *flt4*^{um200}, but it is hereafter referred to as *flt4*$^{Y1226/7\Delta}$. Despite this deletion, we did not observe obvious changes in *flt4* transcript or protein levels, as assessed by whole-mount staining (Fig. 1D). Furthermore, dimerization of the Flt4$^{Y1226/7\Delta}$ cytoplasmic domain induced tyrosine autophosphorylation similar to an Flt4 cytoplasmic domain bearing Y1226/7F point mutations and to wild type (Fig. 1E). Dimerization of Flt4$^{Y1226/7\Delta}$ also resulted in a significant attenuation of basal and induced phosphorylated ERK (pERK) levels in HEK293 cells compared with the wild-type Flt4 cytoplasmic domain, similar to the effect of Y1226/7F mutations (Fig. 1F,G). This effect is similar to previous studies of human FLT4 bearing Y1230/1F mutations (Salameh et al., 2005). Unlike previous studies, we did not observe pAKT induction following Flt4 dimerization, possibly due to the already high levels of AKT phosphorylation in HEK293 cells (Fig. 1F). Together, these observations suggest that the 23 amino acid deletion in *flt4*$^{Y1226/7\Delta}$ mutant embryos can attenuate ERK activation, but does not generally affect Flt4 catalytic activity.

To assess the importance of Y1226/7, we compared phenotypes in *flt4*$^{Y1226/7\Delta}$ mutant embryos with those associated with *vegfc*^{um18}

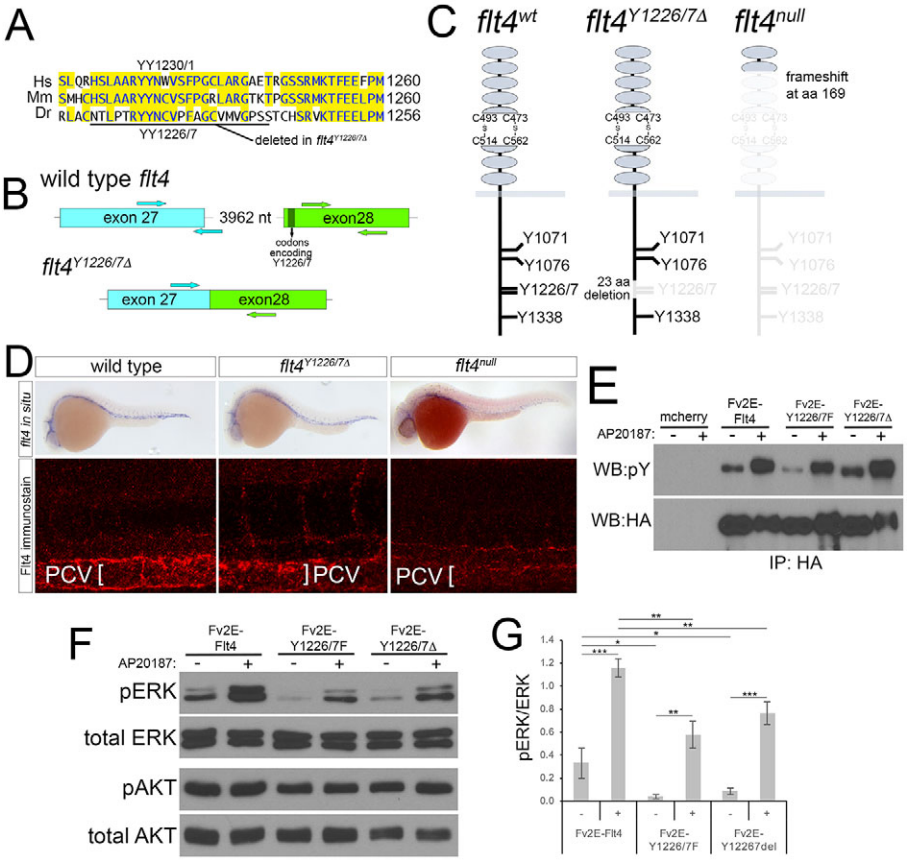

Fig. 1. Targeted deletion of Flt4 Y1226/7. (A) Flt4 cytoplasmic domains from human (Hs), mouse (Mm), and zebrafish (Dr). YY1226/7 and 23 amino acid deletion in *flt4*$^{Y1226/7\Delta}$ mutants are shown. (B) Schematic of wild-type *flt4* and *flt4*$^{Y1226/7\Delta}$ genomic loci. Positions of TALEN pairs in exon 27 and exon 28 are indicated by arrows and codons encoding Y1226/7 are noted. (C) Schematics of wild-type, Flt4$^{Y1226/7\Delta}$ and Flt4^{null} receptors. Residues eliminated by targeted deletions are grayed out. (D) Top: whole-mount *in situ* hybridization using a digoxigenin-labeled antisense *flt4* riboprobe on embryos of the indicated genotype at 25 hpf. Bottom: whole-mount immunostaining using a polyclonal antibody against zebrafish Flt4 at 30 hpf. (E) Immunoprecipitates from human embryonic kidney cells transfected with the indicated constructs and treated with AP20187 to dimerize Fv2E (+), or left untreated (–). Antibodies used for immunoprecipitation (IP) or western blot are indicated. pY, phophotyrosine; HA, hemagglutinin. (F) Western blot analysis of lysates from cells transfected with the indicated construct and treated with AP20187 (+), or left untreated (–). (G) Quantification of pERK/ERK ratio from triplicate western blots (as in F). *P<0.05, **P<0.01, ***P<0.001; error bars are ±s.d.

Development (2016) 143, 3785-3795 doi:10.1242/dev.137901

or *flt4*^{um131} mutations. The *vegfc*^{um18} allele causes a premature stop codon that truncates the Vegfc protein and prevents its secretion, causing fully penetrant defects in lymphatic morphogenesis (Villefranc et al., 2013). The *um131* mutation truncates Flt4 in the extracellular domain (Kok et al., 2015) and causes loss of *flt4* transcript and protein (Fig. 1C,D). Therefore, *flt4*^{um131} is likely to be a null allele and is hereafter referred to as *flt4*^{null}.

flt4$^{Y1226/7\Delta}$ and *flt4*^{null} mutant zebrafish display similar defects in vein and trunk lymphatic development

One of the earliest processes that requires Vegfc/Flt4 signaling is the formation of the primordial hindbrain channel (PHBC), a transient vein that returns cranial circulation to the heart (Covassin et al., 2006). In wild-type embryos, the PHBC forms by sprouting and fusion of two distinct endothelial cell populations, one that originates immediately caudal to the eye, the other near the Duct of Cuvier (Siekmann et al., 2009). Consistent with previous studies (Covassin et al., 2006; Villefranc et al., 2013), nearly all *flt4*^{null} mutant embryos fail to form a complete PHBC by 26 hpf, similar to *vegfc*^{um18} mutants (Fig. 2A,B,G; data not shown). Likewise, *flt4*$^{Y1226/7\Delta}$ mutant embryos displayed PHBC defects at a penetrance similar to the *flt4*^{null} allele (Fig. 2C,G).

We next assessed the severity of lymphatic defects in *flt4* mutant embryos by observing formation of the thoracic duct (TD), which is located immediately ventral to the dorsal aorta in the trunk of wild-type larvae at 5 days post fertilization (dpf; Fig. 2D). In both *flt4*^{null} and *flt4*$^{Y1226/7\Delta}$ mutant embryos we noted a fully penetrant deficit in TD formation at 5 dpf (Fig. 2E,F,H). Both alleles also displayed weaker partially penetrant TD defects in heterozygous embryos (Fig. 2H; data not shown). Similar results were observed in *vegfc*^{um18} mutant embryos, although a much higher proportion of heterozygous embryos displayed TD defects (Fig. 2H).

TD formation entails a complex migratory process in which Prox1-positive endothelial cells sprout from the posterior cardinal vein (PCV) beginning at 30 hpf (Koltowska et al., 2015; Nicenboim et al., 2015; Yaniv et al., 2006). After sprouting dorsally, Prox1-positive lymphatic endothelial cells branch laterally and sprout along the horizontal myoseptum as parachordal cells (PACs). The PACs then sprout ventrally, usually along intersomitic arteries (ISAs) in adjacent somites, to give rise to the TD. During the same developmental window, Prox1-negative venous endothelial cells sprout to form intersomitic veins (ISVs) in parallel and fuse with ISAs, thereby establishing a circulatory network with alternating arterial and venous connections (Isogai et al., 2003). In wild-type embryos at 36 hpf, we observed sprouts emerging from the PCV using Tie2 (Tek) immunostaining and these were absent in *flt4*^{null} and *flt4*$^{Y1226/7\Delta}$ mutant embryos (Fig. 3A-C), suggesting a block in both venous and lymphatic sprouting. Consistent with loss of venous sprouts, both *flt4*^{null} and *flt4*$^{Y1226/7\Delta}$ mutant embryos displayed a significant increase in ISA connections, an effect that was more severe in *vegfc*^{um18} mutants (Fig. 3D). In parallel, we noted a failure to form PACs in both *flt4*^{null} and *flt4*$^{Y1226/7\Delta}$ mutant *Tg(fli1a:egfp)*^{y1} embryos (Fig. 3E-G), suggesting that sprouting of lymphatic progenitors was similarly affected. Accordingly, *flt4*$^{Y1226/7\Delta}$ mutant *Tg(fli1a:egfp)*^{y1} embryos lack Prox1-positive PCV endothelial cells, similar to *vegfc*^{um18} and *flt4*^{null} mutants (Fig. 3H-J; data not shown). In all cases, Prox1 was still apparent in non-vascular tissue (Fig. 3H,I; data not shown). A time course demonstrated that the population of Prox1-positive endothelial cells in the PCV normally expanded from 30 to 38 hpf in wild-type embryos (Fig. 3K), whereas in *flt4* mutants these

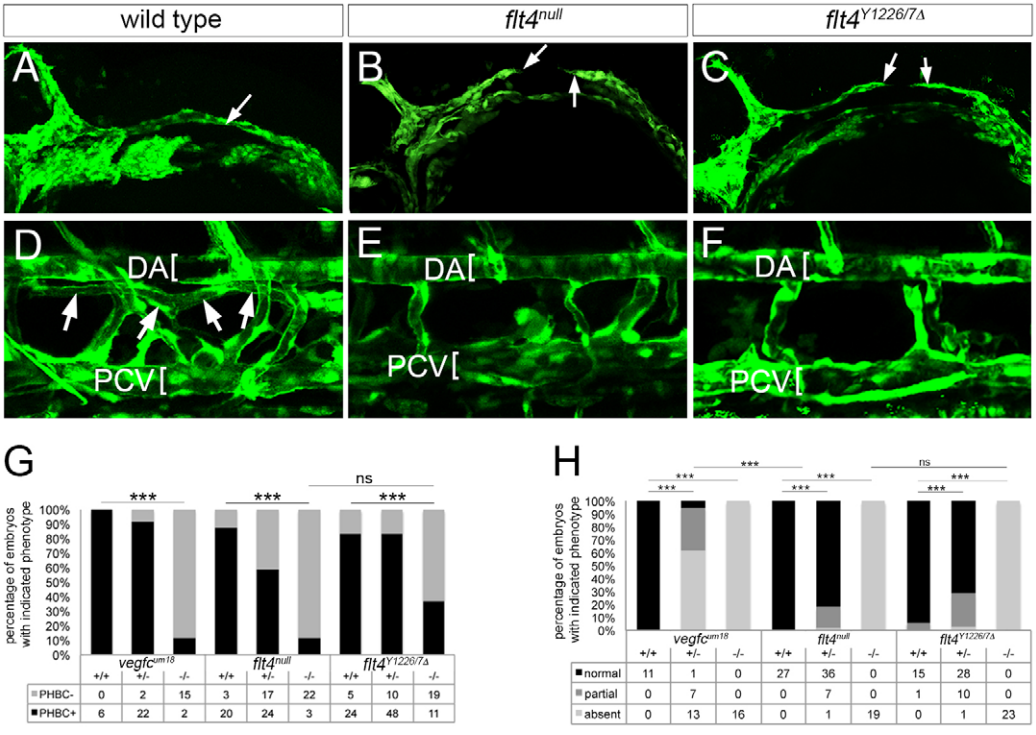

	vegfc^{um18} +/+	vegfc^{um18} +/-	vegfc^{um18} -/-	flt4^{null} +/+	flt4^{null} +/-	flt4^{null} -/-	flt4$^{Y1226/7\Delta}$ +/+	flt4$^{Y1226/7\Delta}$ +/-	flt4$^{Y1226/7\Delta}$ -/-
PHBC-	0	2	15	3	17	22	5	10	19
PHBC+	6	22	2	20	24	3	24	48	11

	vegfc^{um18} +/+	vegfc^{um18} +/-	vegfc^{um18} -/-	flt4^{null} +/+	flt4^{null} +/-	flt4^{null} -/-	flt4$^{Y1226/7\Delta}$ +/+	flt4$^{Y1226/7\Delta}$ +/-	flt4$^{Y1226/7\Delta}$ -/-
normal	11	1	0	27	36	0	15	28	0
partial	0	7	0	0	7	0	1	10	0
absent	0	13	16	0	1	19	0	1	23

Fig. 2. Signaling through Flt4 Y1226/7 is required for vein and lymphatic development. (A-C) Two-photon microscopy of GFP immunostaining in *Tg(fli1a:egfp)*^{y1} embryos of the indicated genotype at 26 hpf; arrows denote fully or partially formed primordial hindbrain channel (PHBC). (D-F) Confocal microscopy of live *Tg(fli1a:egfp)*^{y1} larvae of the indicated genotype at 5 dpf. DA and PCV are denoted by brackets. Thoracic duct (TD) is indicated by arrows in D. (G) Percentage of embryos with the indicated genotype and PHBC formation at 26 hpf. (H) Percentage of embryos of the indicated genotype with TD formation. In G,H, numbers of embryos scored in each category are indicated; ***P<0.001; ns, not significant. In A-F, lateral views, anterior to the left, dorsal is up.

Development (2016) 143, 3785-3795 doi:10.1242/dev.137901

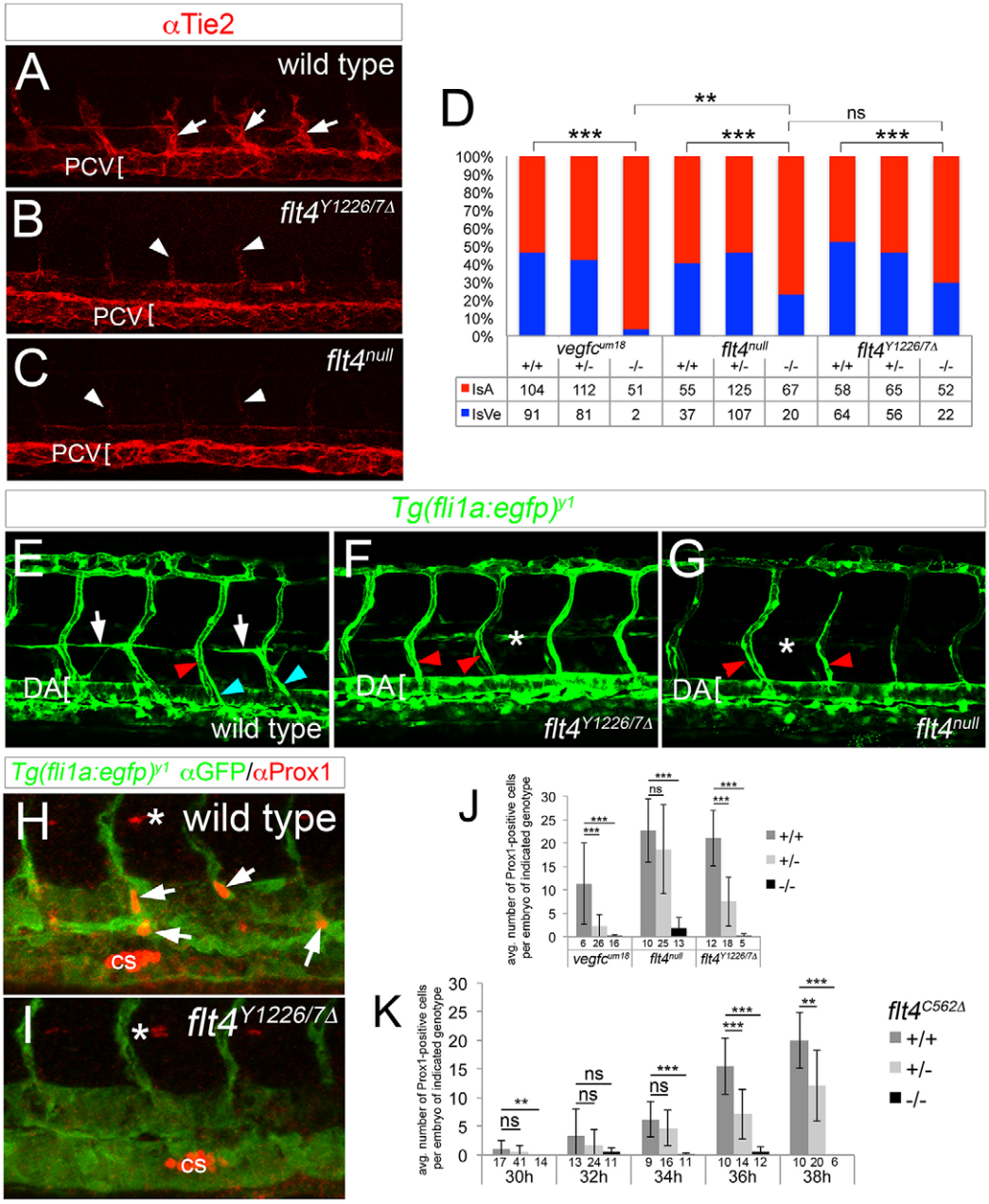

Fig. 3. Signaling through Y1226/7 is essential for initial lympho-venous sprouting and lymphatic differentiation. (A-C) Confocal microscopy of Tie2 immunostaining at 36 hpf. Arrows denote lympho-venous sprouts which give rise to trunk lymphatic and intersomitic vein (ISV) in wild-type embryos; arrowheads indicate intersomitic arteries (ISAs), which display Tie2 faint immunostaining in all embryos. Bracket indicates PCV. (D) Percentage of ISA or ISV connections at 72 hpf in embryos of the indicated genotype as determined by angiography. Total numbers of vessels counted for analysis are indicated. (E-G) Confocal microscopy of live *Tg(fli1a:egfp)^{y1}* embryos of the indicated genotype at 48 hpf. White arrows denote parachordal cells (PACs) in wild-type embryos. Blue and red arrowheads indicate ISVs and ISAs, respectively. Asterisks denote normal position of PACs; occasional fluorescence is observed in non-endothelial cells at the horizontal myoseptum (e.g. panel F). (H,I) Confocal images of Prox1 (red) and GFP (green) immunostaining in *Tg(fli1a:egfp)^{y1}* embryos of the indicated genotype at 36 hpf. Arrows denote Prox1-expressing endothelial cells in lymphatic sprouts; Corpuscle of Stannius (cs) is indicated and asterisk denotes Prox1-positive muscle pioneer. (J,K) Average number of Prox1-positive venous endothelial cells and lymphatic sprouts per embryo of the indicated genotype and at 36 hpf (J) or the indicated stage (K). Total number of embryos scored in each category is indicated on the *x*-axis. (D,J,K) ***P*<0.01, ****P*<0.001; ns, not significant. Error bars are ±s.d. (A-C,E-I) Lateral views, anterior to the left, dorsal is up. Genotype is indicated for each panel.

cells were rarely observed during this period. In this case, we utilized the *flt4^{C562Δ}* allele, which would be expected to disrupt Vegfc binding (Tvorogov et al., 2010) and causes phenotypes similar to *flt4^{null}* (Fig. S1). Together, these results suggest that signaling through Y1226/7 is essential for the initial sprouting of lymphatic and venous endothelial cells, and is required for differentiation and expansion of lymphatic progenitors.

ERK activation is necessary and sufficient to induce differentiation and sprouting of trunk lymphatic vessels

The tyrosines in human FLT4 that are homologous to zebrafish Flt4 Y1226/7 are also important for ERK and AKT activation (Salameh et al., 2005). We observe robust pERK immunostaining in endothelial cells both in the dorsal wall of the PCV, as well as cells sprouting from the PCV, in wild-type *Tg(fli1:egfp)^{y1}* embryos

Development (2016) 143, 3785-3795 doi:10.1242/dev.137901

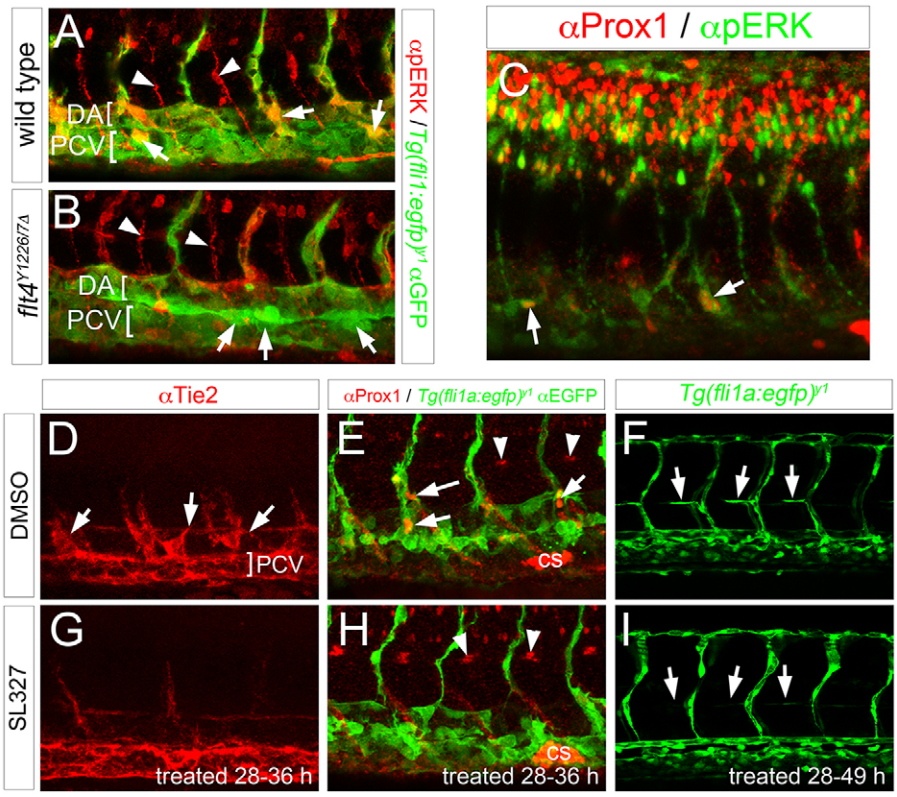

Fig. 4. ERK signaling is essential for trunk lymphatic morphogenesis and differentiation. (A-I) Confocal images; lateral views, anterior to the left, dorsal is up. (A,B) pERK (red) and GFP (green) immunostaining in *Tg(fli1a:egfp)^{y1}* embryos of the indicated genotype at 34 hpf. Arrows denote pERK-positive lympho-venous sprouts, arrowheads indicate pERK staining in motor neurons. Brackets indicate DA and PCV. (C) Prox1 (red) and pERK (green) immunostaining in a wild-type embryo at 38 hpf. Arrows denote endothelial cells that are positive for Prox1 and pERK in lymphatic sprouts or dorsal wall of PCV. (D-I) Embryos treated with DMSO (D-F) or 15 µM SL327 (G-I). Treatment time is indicated. (D,G) Tie2 immunostaining; arrows denote lympho-venous sprouts, PCV indicated by bracket. (E,H) Prox1 (red) and GFP (green) immunostaining of *Tg(fli1a:egfp)^{y1}* embryos at 36 hpf; arrows denote Prox1-positive lymphatic sprouts, arrowheads indicate muscle pioneers and Corpuscle of Stannius (cs) is indicated. (F,I) Live *Tg(fli1a:egfp)^{y1}* embryos at 49 hpf. Arrows indicate parachordal cells, or absence thereof.

(Fig. 4A). By contrast, pERK staining was absent from the PCV in *flt4$^{Y1226/7\Delta}$* mutant siblings, but unaffected in non-endothelial cells (Fig. 4B). Furthermore, we find that Prox1 and pERK colocalize in lymphatic progenitors in the dorsal wall of and sprouting from the PCV (Fig. 4C). These observations suggest that ERK activation may be essential for lymphatic and venous sprouting downstream of Flt4. Accordingly, treatment with SL327 (a MEK inhibitor) beginning at 28 hpf to block ERK phosphorylation (Fig. S2A,B) prevented lympho-venous sprouting (Fig. 4D,G; we use the term 'lympho-venous' to include all sprouts emanating from the PCV because Tie2 immunostaining cannot distinguish between lymphatic and venous sprouts). In addition, ERK inhibition prevented the appearance of Prox1-positive endothelial cells in the PCV and blocked PAC formation in *Tg(fli1a:egfp)^{y1}* embryos (Fig. 4E,H,F,I). We could not assess TD formation as prolonged SL327 treatment led to loss of circulation and severe non-vascular defects at later stages (data not shown). In contrast to SL327, AKT inhibition did not affect Prox1 expression, lympho-venous sprouting, or PAC formation (Fig. S2C-F; data not shown).

To determine if ERK activation was sufficient to drive lymphatic sprouting and differentiation in a cell-autonomous manner in the absence of Vegfc/Flt4, we transiently expressed activated Map2k2b (actMap2k2b) in endothelial cells of *flt4$^{C562\Delta}$* mutant embryos using the GAL4/UAS system (Fig. 5A). In this case, we utilized transiently injected Tol1 transposons (Koga et al., 2008) to avoid mobilizing the *Tg(cdh5:gal4ff)^{mu101}* transgene, which is flanked by Tol2 direct repeat elements (Bussmann et al., 2011). *flt4$^{C562\Delta}$;Tg(cdh5:gal4ff)^{mu101}* mutant embryos injected with a control Tol1 transgene did not form lympho-venous sprouts and failed to induce Prox1 expression in the PCV while displaying robust endothelial-expressed nlstdTomato (Fig. 5B,B′). An activated Akt transgene also failed to rescue Prox1 expression or venous sprouting (Fig. 5C, C′; data not shown; 0 Prox1-positive cells out of 501 transgene-expressing cells in 24 embryos). By contrast, actMap2k2b rescued Prox1 expression and lymphatic sprouting in the PCV of *flt4$^{C562\Delta}$* mutant embryos (Fig. 5D,D′; Fig. S2G). Taken together, these results demonstrate that activation of ERK is sufficient downstream of Flt4 to initiate lymphatic sprouting and differentiation in the PCV.

Signaling through Flt4 Y1226/7 is dispensable for facial lymphatic formation and function

The lymphatic system maintains fluid homeostasis by collecting interstitial fluid and returning it to the circulatory system. Consequently, perturbations to lymphatic morphogenesis prevent interstitial fluid collection and lead to lymphedema. Indeed, both *vegfc^{um18}* and *flt4^{null}* mutant larvae displayed edema around the digestive tract, heart and eyes and failed to inflate their swim bladder by 5 dpf, whereas wild-type larvae were normal (Fig. 6A-C). These defects were observed at nearly full penetrance and resulted in poor adult survival (Fig. 6E; data not shown). Despite their failure to form a TD (Fig. 2F,H), *flt4$^{Y1226/7\Delta}$* mutants were indistinguishable from wild type until 10 dpf (Fig. 6A,D,E) and were viable and fertile as adults (data not shown). These results suggest that the *flt4^{null}* and *flt4$^{Y1226/7\Delta}$* alleles display distinct effects on lymphatic function and that TD formation is dispensable for early lymphatic function.

Because trunk lymphatic defects were the same in *flt4^{null}* and *flt4$^{Y1226/7\Delta}$* mutants, yet overt lymphedema was only observed with complete loss of *flt4*, we investigated whether this was due to distinct effects on facial lymphatic development (Okuda et al., 2012). Facial lymphatic progenitors sprout from the common cardinal vein (CCV) to fuse with lymphatic endothelial cells that emerge from the primary head sinus (PHS) giving rise to an initial facial lymphatic vessel (FLV; see Fig. S3; Okuda et al., 2012). As in the PCV, lymphatic endothelial progenitors emerging from the

Development (2016) 143, 3785-3795 doi:10.1242/dev.137901

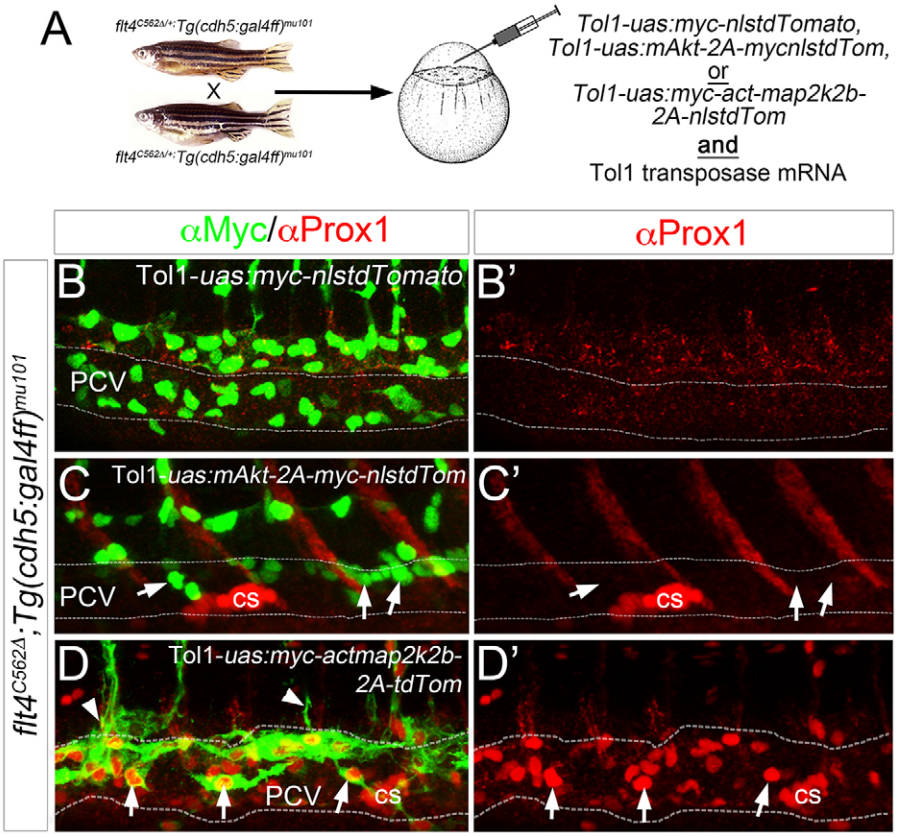

Fig. 5. ERK activation rescues early lymphatic morphogenesis and differentiation in the absence of Flt4 signaling. (A) Schematic depicting injection strategy for rescue experiments. (B-D′) Confocal microscopy of *Tg(cdh5:gal4ff)*^{mu101};*flt4*$^{C562\Delta}$ mutant embryos injected with Tol1-*uas:myc-nlstdTomato* (B), Tol1-*uas:mAkt-2a-myc-nlstdTomato* (C) or Tol1-*uas:myc-actmap2k2b-2a-tdTomato* (D) along with mRNA encoding Tol1 Transposase. (B-D) Overlay of Prox1 (red) and Myc (green) immunostaining to visualize transgene expression in injected embryos at 38 hpf. Arrows indicate transgene-expressing cells; arrowheads indicate transgene-expressing cells that are sprouting from the PCV. (B′-D′) Prox1 immunostaining (red) in same injected embryos as in B-D. Corpuscle of Stannius (cs) is indicated. Dashed lines outline the PCV.

CCV and PHS are positive for Prox1 (Fig. 7A,D). However, we did not observe pERK immunostaining in CCV endothelial cells at the time during which Prox1-positive lymphatic progenitors are beginning to sprout, and *flt4*^{null} mutants appeared indistinguishable from wild type in this regard (Fig. S4A,B). Furthermore, numbers of Prox1-positive endothelial cells were unchanged in embryos mutant for either *flt4*^{null} or *flt4*$^{Y1226/7\Delta}$ compared with wild-type siblings (Fig. 7B,C,E-G). In addition, Prox1 expression in CCV endothelial cells was not affected by treatment with 15 µM SL327, although these same embryos display loss of Prox1 in trunk PCV endothelial cells (Fig. S4C-G).

To visualize facial lymphatic morphology in *vegfc* and *flt4* mutants, we relied on the *Tg(lyve1b:DsRed2)*^{nz101} transgenic line (Okuda et al., 2012). Because developing facial lymphatics lie directly lateral to the PHS, we color-coded vertical projections from confocal stacks based on depth. This approach allowed us to distinguish more easily the PHS from the lateral facial lymphatic (LFL), otolithic lymphatic vessel (OLV) and the initial budding of lymphatic branchial arch (LAA) sprouts (Fig. 7H). In all *Tg(lyve1b:DsRed2)*^{nz101} embryos mutant for either *vegfc*^{um18} or *flt4*^{null}, we observed severe truncation of the LFL and a failure to form LAA buds or the OLV, whereas formation of the PHS and posterior cerebral vein (PCeV) was unaffected (Fig. 7I-L). By contrast, nearly all *flt4*$^{Y1226/7\Delta}$ mutant embryos exhibited formation of the LFL and LAA buds, although the OLV appeared to be delayed (Fig. 7K,L). Interestingly, treatment with SL327 from 28 to 50 hpf blocked facial lymphatic morphogenesis, although initial sprouting of lymphatic progenitors from the CCV was apparent (Fig. S3H,I).

The facial lymphatic network should retain a connection to the vascular system to allow excess fluid to return back into circulation. Accordingly, we observed perfusion of the LFL with Qdots following angiography, but not with *gata1:dsRed*-expressing red blood cells (Fig. 7M). By contrast, both red blood cells and Qdots were readily apparent in the PHS (Fig. 7M). In *vegfc*^{um18} and *flt4*^{null} mutant embryos, we observed incomplete perfusion of the LFL compared with wild-type siblings (Fig. 7N-P) consistent with reduced formation of the facial lymphatics. By contrast, *flt4*$^{Y1226/7\Delta}$ mutant embryos were indistinguishable from wild type (Fig. 7N,Q). Taken together, these results demonstrate distinct signaling requirements for facial and trunk lymphatic development and suggest that the facial lymphatics are the first functional lymphatic network in the zebrafish.

DISCUSSION

In this study, we have applied TALENs to generate a *flt4* allele that affects signaling through tyrosine residues previously implicated in AKT and ERK activation in cell culture (Salameh et al., 2005). By comparing phenotypes associated with deletion of Y1226/7 with that of a null *flt4* mutant we find evidence of distinct genetic requirements for Vegfc/Flt4 signaling in the development of the facial and trunk lymphatic networks. In the trunk, Flt4 signals through ERK to drive progenitor differentiation, expansion and sprouting at the earliest stages of lymphatic development. These observations are consistent with recent findings that demonstrate an important role for Vegfc in the direct induction of Prox1 expression in lymphatic progenitors within the posterior cardinal vein, as well as their subsequent expansion (Koltowska et al., 2015). Our results further show that ERK plays an essential role downstream of Vegfc and Flt4 in this crucial early step in lymphatic development.

Despite the early role for a Vegfc/Flt4/ERK signaling cascade in trunk lymphatic development, we do not observe a similar genetic requirement for Y1226/7 in facial lymphatics. Recent work has

Development (2016) 143, 3785-3795 doi:10.1242/dev.137901

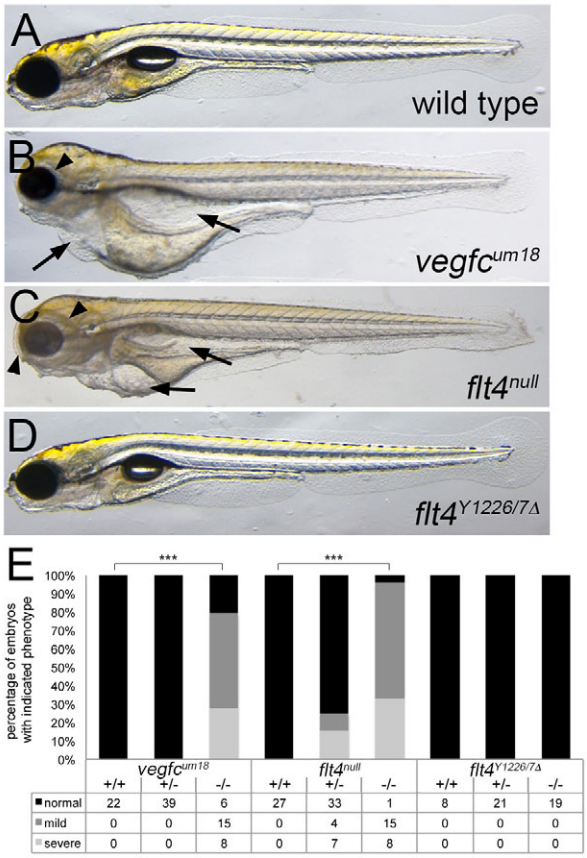

Fig. 6. Signaling through Flt4 Y1226/7 is dispensable for normal lymphatic function. (A-D) Transmitted light images of live zebrafish larvae at 10 dpf (A,D) or 5 dpf (B,C). Genotype is indicated in each panel. Lateral views, anterior to the left, dorsal is up. Arrows denote edema surrounding the intestinal tract and heart, arrowheads indicate edema surrounding the eyes. (E) Proportion and numbers of larvae of the indicated genotype exhibiting edema at 5 dpf for *vegfc*^{um18} and *flt4*^{um131} or 10 dpf for *flt4*$^{Y1226/7\Delta}$. ***P<0.001.

demonstrated a differential requirement for *vegfd* (*figf*) and *vegfc*, as well as chemokine receptor signaling, between facial and trunk lymphatic vessels (Astin et al., 2014). Thus, our observations are consistent with the likelihood that there is anatomical heterogeneity in lymphatic endothelial progenitors during early embryonic development. Unlike the PCV, ERK activation does not appear in Prox1-positive cells within the CCV. However, later sprouting of facial lymphatic vessels is blocked by SL327 treatment, suggesting a later role for ERK, albeit independent of signaling through Flt4 Y1226/7. Interestingly, Prox1 is retained in the CCV even in *flt4*^{null} embryos, suggesting that initial lymphatic specification is independent of both Vegfc and ERK in this particular anatomical location. This phenotype is similar to that observed in mouse, where loss of Vegfc blocks sprouting of lymphatic progenitors from the cardinal vein, but initial Prox1 expression appears normal in these cells (Karkkainen et al., 2004). Thus, several of the discrepancies that have been noted between Vegfc signaling mutants in zebrafish and mouse embryos might be due to anatomical distinctions between lymphatic networks rather than species-specific differences. In any case, it will be important to identify the molecular basis of heterogeneity in these lymphatic networks to gain a better understanding of the requisite signaling effectors responsible for their development in different anatomical locations.

The differential requirement for the trunk and facial lymphatic networks strengthens the likelihood that the Y1226/7 deletion specifically affects particular downstream effectors, rather than acting as a general hypomorphic allele that simply reduces overall Flt4 signaling output. If the latter were true, we would expect intermediate levels of expressivity and penetrance, especially when considering the trunk lymphatic and lymphedema phenotypes. Rather, we observe a stark difference in phenotypic penetrance when comparing the *flt4*^{null} and *flt4*$^{Y1226/7\Delta}$ alleles: whereas both alleles behave identically regarding trunk lymphatic development, there are clear distinctions in facial lymphatic morphogenesis and function, for which signaling through the domain encoding Y1226/7 appears to be dispensable. Coupled with our demonstration of normal transcript and protein expression levels, and no general effect on autophosphorylation, these observations provide strong evidence that the *flt4*$^{Y1226/7\Delta}$ allele is specifically affecting downstream Flt4 signaling. However, given the nature of the allele, we cannot rule out the possibility that this effect may not be dependent on tyrosines 1226/7, but rather relies on other residues within this domain. Moving forward, it will be important to develop more robust approaches to establish point mutations using available genome-editing tools in zebrafish.

In human FLT4, tyrosines homologous to zebrafish Y1226/7 are required for activation of both AKT and ERK in endothelial cell culture (Salameh et al., 2005). However, our chemical inhibition and autonomous transgenic rescue experiments suggest that activation of ERK, but not AKT, is necessary and sufficient to induce trunk lymphatic development in the zebrafish. It remains a possibility that signaling through AKT may be utilized downstream of Flt4 at later stages of lymphatic morphogenesis or maintenance. Indeed, signaling through the phosphoinositide 3-kinase (PI3K) pathway, an essential upstream activator of AKT, has been implicated in both mice and humans at later stages of lymphatic morphogenesis and maintenance, and in an organ-specific manner (Boscolo et al., 2015; Mouta-Bellum et al., 2009). Thus, although these studies suggest that it is likely that AKT plays an important role in lymphatic development, our findings rule out this effector during the earliest steps of trunk lymphatic development. Rather, Vegfc signals specifically through ERK to initiate sprouting and differentiation of trunk lymphatic progenitors in the zebrafish. Generation of targeted alleles that specifically disrupt PI3K signaling will be helpful to improve our understanding of the role of this pathway in zebrafish lymphatic morphogenesis.

Consistent with our findings, several observations in mouse have provided convincing indirect evidence that implicate ERK in lymphatic morphogenesis and differentiation. Mice lacking both *Spred1* and *Spred2*, or deficient in the RasGAP Rasa1, all of which are negative regulators of the MEK/ERK signaling cascade, display increased numbers of lymphatic endothelial cells (Lapinski et al., 2012; Taniguchi et al., 2007). Moreover, lymphatic endothelial cells in these mice exhibit ectopic ERK signaling and abnormal lymphatic function. Similarly, inducible endothelial-driven expression of an activated Raf1S259A transgene, which can lead to increased ERK activation, induces ectopic lymphatic formation in mouse. In this case, Raf1S259A also drives expression of lymphatic regulators Prox1 and Sox18 in endothelial cells *in vivo* (Deng et al., 2013). This finding is consistent with our results that demonstrate that ERK activation can potently induce Prox1 expression and induce lymphatic sprouting downstream of Flt4. The similarity between *flt4*$^{Y1226/7\Delta}$, *flt4*^{null} and *vegfc*^{um18} embryos further suggests that ERK activation occurs downstream of Vegfc and Flt4, rather

Development (2016) 143, 3785-3795 doi:10.1242/dev.137901

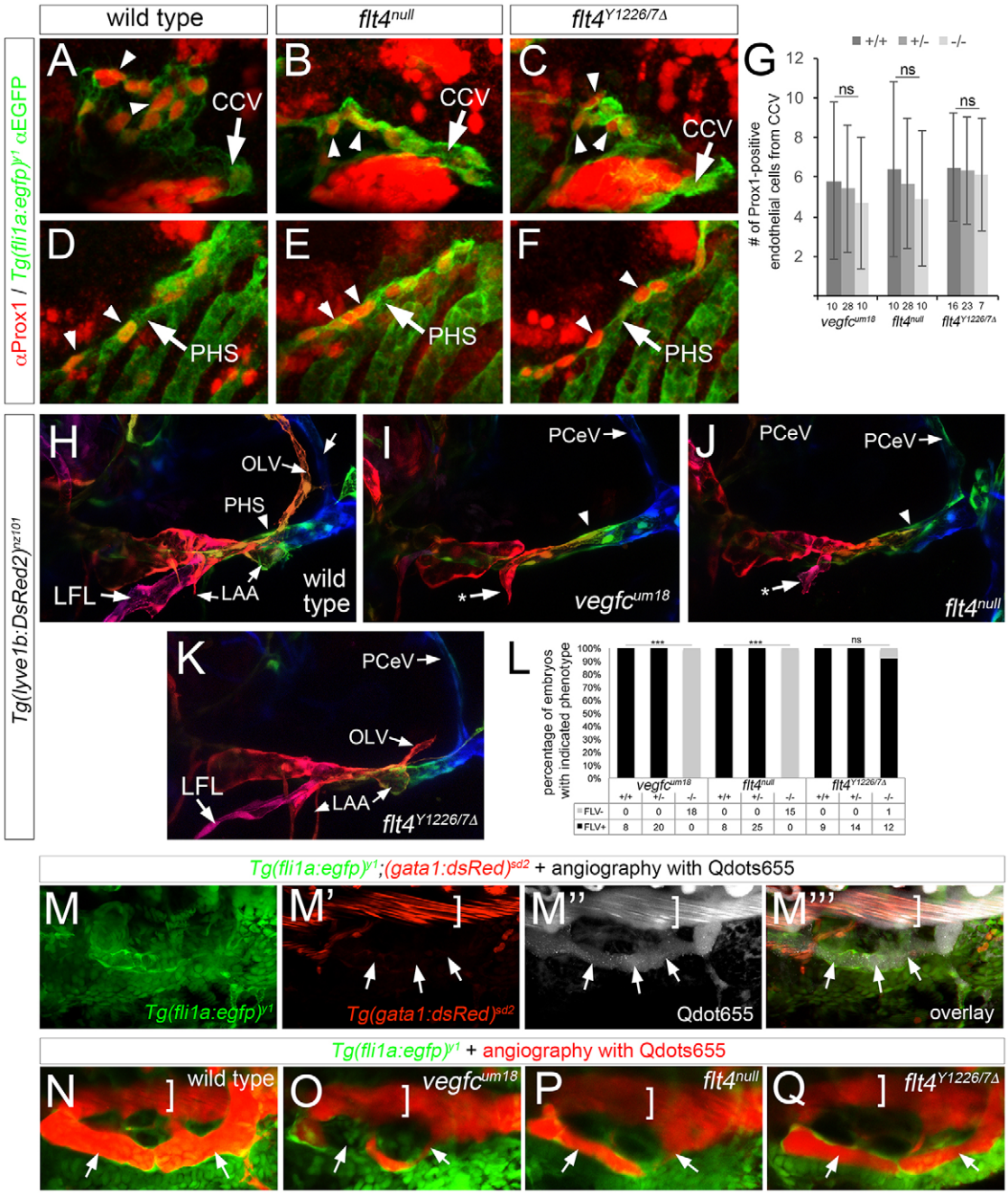

Fig. 7. Signaling through Flt4 Y1226/7 is dispensable for facial lymphatic formation and function. (A-F) Confocal images of *Tg(fli1a:egfp)^{y1}* embryos at 36 hpf of the indicated genotype immunostained with antibodies against Prox1 in red and GFP in green. (A-C) Arrowheads denote Prox1-positive endothelial cells in facial lymphatic sprout (FLS) emerging from the common cardinal vein (CCV, indicated by an arrow). (D-F) Prox1-positive endothelial cells within primary head sinus (PHS, indicated by an arrow) at 36 hpf denoted by arrowheads. (G) Quantification of Prox1-positive cells from the CCV at 36 hpf; ns, not statistically significant; error bars are ±s.d. (H-K) Confocal images of live *Tg(lyve1b:dsRed2)^{nz101}* embryos of the indicated genotype at 4 dpf; pseudocoloring is based on depth: red is surface, green and blue are deeper. Lateral facial lymphatic (LFL), otolithic lymphatic vessel (OLV), posterior cerebral vein (PCeV) and forming lymphatic aortic arches (LAA) are indicated. Arrowhead denotes dorsal wall of the primary head sinus (PHS), which is pseudocolored green. Arrows indicated by asterisks denote stunted LFL. (A-F,H-K) Lateral views, anterior to the left, dorsal is up. (L) Percentage of embryos of the indicated genotype with FLV formation. Numbers of embryos scored in each category are indicated; ***P<0.001; ns, not significant. (M-Q) Dorsal views, anterior to the left. (M-M‴) Live wild-type *Tg(fli1a:egfp)^{y1};(gata1:dsRed2)^{sd2}* embryo at 4 dpf subjected to microangiography with Qdots655 (gray). Arrows denote Qdot perfusion of FLV, bracket indicates PHS lumen. (N-Q) Confocal images of live *Tg(fli1a:egfp)^{y1}* embryos at 4 dpf of the indicated genotype subjected to microangiography with Qdots655 (red). Arrows denote FLV, bracket indicates the lumen of the PHS.

than being targeted by other lymphatic RTKs. Thus, our studies provide a crucial link to observations in mouse and demonstrate that Vegfc signaling through Flt4 activates ERK to initiate lymphatic morphogenesis and differentiation.

The discovery and initial characterization of an early lymphatic system in zebrafish was only made a decade ago (Yaniv et al., 2006). The majority of subsequent work has focused on the development of and genetic signals that govern formation of the TD, an

Development (2016) 143, 3785-3795 doi:10.1242/dev.137901

anatomically conserved lymphatic vessel (Mulligan and Weinstein, 2014). With the advent of lymphatic- and vein-specific transgenic zebrafish, more recent work has described the development of a facial lymphatic network between 2 and 5 dpf (Okuda et al., 2012). Given that *flt4*$^{Y1226/7\Delta}$ mutants specifically lack a trunk lymphatic network, our analysis would suggest that the facial lymphatic network, but not the TD, is the first functional lymphatic vessel during zebrafish development. Moving forward, it will be important to apply similar genetic approaches to dissect the distinct signaling requirements that pattern these lymphatic networks.

MATERIALS AND METHODS

Zebrafish and maintenance

Zebrafish were handled according to approved University of Massachusetts Medical School Institutional Animal Care and Use Committee protocols. *Tg(fli1a:egfp)*^{y1}, *Tg(cdh5:gal4ff)*^{mu101}, *Tg(kdrl:egfp)*^{la116}, *Tg(gata1:DsRed)*^{sd2} and *Tg(lyve1b:DsRed2)*^{nz101} are described elsewhere (Bussmann et al., 2011; Choi et al., 2007; Lawson and Weinstein, 2002; Okuda et al., 2012; Traver et al., 2003). The *vegfc*^{um18} and *flt4*^{null} alleles have been described previously (Kok et al., 2015; Villefranc et al., 2013).

Knockout generation and genotyping

To delete Y1226/7, we designed TALENs to the following sites: exon 27, 5p target: 5′-CACAAGAGGAGATCAGAT-3′, 3p target: 5′-GTTGCTGTACCGTGTTGGC-3′, separated by a 16-nt spacer; exon 28, 5p target: 5′-GCCGTTTGCTGGCTGTGTGA-3′, 3p target: 5′-TCACTCGAGAATGACATGTG-3′ separated by a 16-nt spacer. To introduce mutations in *flt4* at C562, we targeted the following sites in exon 12 using TALENs: 5p target: 5′-GCCAGTGTGCCAGCTAT-3′, and 3p target: 5′-CTTTTCCCACTTTGTTCT-3′, separated by a 17-nt spacer. TALENs were constructed as described elsewhere (Kok et al., 2014). TALEN mRNAs were injected into wild-type embryos at the one-cell stage. To establish the *Y1226/7Δ* allele, exon 27 and exon 28 TALEN pairs were co-injected. Founders were identified as previously described (Meng et al., 2008). For C562, we identified a founder bearing a 9-nt deletion (*flt4*$^{C562\Delta}$). For Y1226/7, we identified a founder bearing a 4031-nt deletion that eliminates 23 amino acids encoded by exons 27 and 28, including codons encoding Y1226/7. Each founder was outcrossed to *Tg(fli1a:egfp)*^{y1} adults and heterozygous carriers for *flt4*$^{C562\Delta}$ or *flt4*$^{Y1226/7\Delta}$ were confirmed by sequencing. All embryos were genotyped following all phenotypic analysis. Genotyping for *C562Δ* was performed by PCR using the following primers: 5′-tgtcggccgtgtggttattcag-3′ and 5′-agcatgaaactcactggttacgtag-3′, followed by digestion with *Mwo*I (NEB), which cuts the mutant allele. Genotyping for *Y1226/7Δ* was carried out using two primer sets, one (5′-tcagattggcctgcacatgtc-3′ and 5′-ctggaggacgtaatcgacgtacatg-3′) recognizes *Y1226/7Δ* allele and the other (5′-atcagattggcctgcaacacac-3′ and 5′-ccggcttacatagctgagaaggctag-3′) recognizes wild-type allele. *flt4*^{um131} genotyping was carried out using 5′-ttcagaacttataggcagctgaac-3′ and 5′-catttcctttggcttggaaa-3′ followed by Taqα1 (NEB), which digests wild type but not the mutant allele. Owing to the presence of a single nucleotide polymorphism at the *flt4*^{um131} target site in some wild-type fish that eliminated the Taqα1 site, we also performed KASP genotyping assay (LGC Company) using the following primers: wild-type allele FAM primer (5′-atcttcataacagactctgaaacacac-3′), *um131* allele HEX primer (5′-catcttcataacagactctgaaacacat-3′) and common primer (5′-gtcaggatctgaaaccagacatggta-3′). KASP assays were performed on a StepOnePlus Real-Time PCR machine (Life Technologies) using the primers above with 2× KASP Master Mix High ROX V4.0 (LGC Company).

Plasmid construction

A multisite Gateway destination cassette (attR4-*ccdb-cam*^{r}-attR3) followed by a polyadenylation sequence and flanked by Tol1 direct repeats (Koga et al., 2008) was synthesized in pUC57amp (Genewiz) and is referred to as pToneDest. A cDNA encoding full-length Tol1 transposase (Koga et al., 2008) and a polyadenylation sequence was synthesized in pUC57 downstream of a T7 promoter and is referred to as pToneTpase. 6x myc-tagged tdTomato with a nuclear localization signal (MPKKKRKV) was subcloned into pDONR221 or pDONRP2P3 using BP clonase II (Invitrogen) and are referred to as pME-*myc-nlstdTomato* and p3E-*2a-myc-nlstdTomato*, respectively. An activated myc-tagged form of MEK was generated from zebrafish *map2k2b* by mutating serines 211 and 225 to aspartic acid (Schramek et al., 1997) by PCR, followed by BP cloning to generate pME-*myc*-act-*map2k2b*. For expression constructs, p5E-*uasE1b* (Kwan et al., 2007), pME-*myc-nlstdTomato*, pME-*myc-act-map2k2b* or pME-*mAkt* (Covassin et al., 2009) and an empty p3E-mcs-1, p3E-*2a-myc-nlstdTomato* or p3E-*2a-tdTomato* were cloned into pToneDest using LR clonase II (Invitrogen) to give pTol1:*uas-myc-nlstdTomato*, pTol1:*uas-myc-act-map2k2b-2a-tdTomato* and pTol1:*uas-mAkt-2a-myc-nlstdTomato*. To test Flt4 autophosphorylation, cDNA encoding the Flt4 intracellular domain (amino acids 820-1354) was ligated into the *Spe*I site of pC$_4$M-F$_v$2E (Ariad) and subcloned into pDONR221 (pME-*F$_v$2E-flt4-HA*). This construct was used to generate F$_v$2E-*flt4*$^{Y1226/1227F}$ by substituting tyrosine 1226 and 1227 with phenylalanine or by deleting amino acids 1220-1242 to generate F$_v$2E-*flt4*$^{Y1226/7\Delta}$ (pME-*F$_v$2E-flt4*$^{Y1226/1227F}$*-HA* and pME-*F$_v$2E-flt4*$^{Y1226/7\Delta}$*-HA*, respectively). Each pME-*F$_v$2E-flt4* plasmid, along with p3E-HA, was LR cloned into pCS-Dest2 (Villefranc et al., 2007) to generate pCS2-*F$_v$2E-flt4-HA*, pCS2-*F$_v$2E-flt4*$^{Y1226/1227F}$*-HA* and pCS2-*F$_v$2E-flt4*$^{Y1226/7\Delta}$*-HA*. All plasmids are available at Addgene.org (https://www.addgene.org/browse/article/14538/).

Rescue injections

Embryos derived from an incross of *flt4*$^{C562\Delta/+}$*;Tg(cdh5:gal4ff)*^{mu101} carriers were injected with 20 pg of *pTol1:uas-myc-nlstdTomato*, pTol1:*uas-mAkt-2a-myc-nlstdTomato* or *pTol1:uas-myc-act-map2k2b-2a-tdTomato* with 50 pg Tol1 *transposase* mRNA. Injected embryos were incubated in egg water with 1× phenylthiourea (PTU) until 38 hpf then fixed for immunostaining (see below). Tol1 *transposase* mRNA was synthesized using T7 polymerase (mMessageMachine, Ambion) following *Not*I digestion of pToneTpase.

Inhibitor treatment

To block phosphorylation and activation of ERK1/2, embryos were incubated in egg water with 1× PTU and 15 µM SL327 (EMD Millipore) from 28 hpf to 36 hpf or 49 hpf. To block phosphorylation of AKT1/2/3, we used 25 µM MK2206 (Santa Cruz). Lysates were prepared from embryos treated with 1, 10, 25 and 100 µM MK2206 or DMSO from 24 hpf to 28 hpf and separated by 10% SDS-PAGE, followed by western blotting. Blots were incubated with antibodies against phospho-AKT (Ser473) XP Rabbit monoclonal antibody (1:2000; #4060, Cell Signaling) and pan AKT Rabbit monoclonal antibody (1:5000; #4691, Cell Signaling). Phosphorylation level of AKT was measured using ImageJ.

Cell culture and dimerization assay

pCS-*myc-mCherry*, pCS2-*F$_v$2E-flt4-HA-2a-tdTomato*, pCS2-*F$_v$2E-flt4*$^{Y1226/1227F}$*-HA-2a-tdTomato* and pCS2-*F$_v$2E-flt4*$^{Y1226/7\Delta}$*-HA-2a-tdTomato* were transfected in HEK293T cells with DMEM/10% fetal bovine serum media on 10 cm dishes using Effectene (Qiagen). Cells were treated for 30 min with 500 nM AP20187 (Ariad) to induce F$_v$2E dimerization or ethanol as negative control, and lysed using RIPA buffer (150 mM NaCl, 50 mM Tris-HCl pH 8.0, 1% NP-40, 0.1% SDS) with protease and phosphatase inhibitors (Roche and Sigma, respectively). Lysates were immunoprecipitated using monoclonal anti-HA antibody (H3663, Sigma) and blotted with anti-phospho-Tyrosine (4G10, EMD Millipore), -HA, -panERK, -pERK, -panAKT or -pAKT antibody.

In situ hybridization and immunostaining

In situ hybridization was carried out using *flt4* riboprobe as previously described (Siekmann and Lawson, 2007). GFP immunostaining was performed as previously described (Covassin et al., 2006). Immunostaining for Prox1, ERK and Flt4 was performed using a protocol described elsewhere (Nicenboim et al., 2015) with some modifications. Briefly, embryos were permeabilized sequentially with water and PBSTw (PBS containing 0.1% Tween 20)/1% Triton X-100. For antigen retrieval, embryos were incubated in citrate buffer (0.1 M sodium citrate dehydrate/0.05% Tween 20, pH 6.0) for 20 min at 98°C. The following antibodies and dilutions were used: 1:5000

Development (2016) 143, 3785-3795 doi:10.1242/dev.137901

rabbit anti-Flt4 polyclonal antibody (Villefranc et al., 2013), 1:1000 anti-Prox1 antibody (ab11941, Abcam) or 1:250 phospho-ERK1/2 (Thr202/Tyr204) XP rabbit monoclonal antibody (#4370, Cell Signaling) with 1:500 monoclonal anti-GFP antibody (sc-9996, Santa Cruz) or 1:500 monoclonal anti-Myc antibody (9E10, Sigma) in blocking buffer (PBSTw/0.1% Triton X-100/2% DMSO/5% bovine serum albumin/1% goat serum). GFP and Myc were detected with goat anti-mouse IgG(H+L)-Alexa488 (A11029, Thermo Fisher Scientific). For Tie2 staining, embryos were fixed with 4% paraformaldehyde in PBS (PFA/PBS) overnight at 4°C, quenched with 3% H_2O_2 in methanol and stored in methanol at −20°C until use. Embryos were treated with 30 µg/ml proteinaseK (NEB) in PBSTw (PBS/0.1% Tween 20) for 1 min and fixed in 4% PFA/PBS. After blocking with PBSTw/2% blocking reagent (Roche), embryos were incubated with 1:100 goat anti-zTie2 antibody (AF928, R&D Systems) overnight at 4°C, washed with PBSTw, and incubated with 1:5000 ZyMAX rabbit anti-goat IgG(H+L)-HRP (81-1620, Thermo Fisher Scientific) overnight at 4°C. Embryos were washed with PBSTw, then PBS, and incubated with 1:50 tyramide-Cy3 in 1× amplification diluent (PerkinElmer) for detection. For simultaneous detection of Prox1 and pERK1/2, embryos were immunostained with Prox1 antibody followed by incubation in citrate buffer for 20 min at 98°C to denature the primary and secondary antibodies. After blocking, embryos were incubated in pERK1/2 (Thr202/Tyr204) XP rabbit monoclonal antibody overnight at 4°C, then with goat anti-rabbit IgG(H+L)-HRP, and signals was detected with tyramide-FITC (PerkinElmer).

Imaging

Embryos were placed in 1.5% low melt agarose on a 35 mm glass-bottomed culture dish filled with egg water. For live embryos, 1× tricaine was included. Images were acquired using a Zeiss LSM710 equipped with a W Plan-APOCHROMAT 20×/1.0 DIC D=0.17 M27 70 mm objective lens. GFP, Alexa488 or FITC, and Cy3 were simultaneously excited at 488 nm and 561 nm of confocal lasers, respectively. Emissions were split by a MBS 488/561/633 beam splitter and captured with two detection ranges (ch1: 493-536 nm, ch2: 576-685 nm). PHBC formation was imaged using a two-photon Chameleon Ti:Sapphire pulse laser (Coherent) at 900 nm through a 500-550 nm band pass filter into a BiG detector. Angiography using Qdot655 was performed as previously described (Siekmann and Lawson, 2007). Vertical projections of image stacks were assembled and quantified using ImageJ with Fiji or Imaris ver.7 (Bitplane). For depth colorization of the facial lymphatic stacks, we utilized the Temporal Color Code function in Fiji.

Phenotypic analysis

PHBC formation was scored in *Tg(fli1a:egfp)*^{y1} embryos between 25 and 26 hpf on a M165FC microscope (Leica), or in two-photon images following GFP immunostaining. For quantification of intersegmental artery and vein connections at 72 hpf, image stacks were surface-rendered using Imaris and assessed for connection to the dorsal aorta or PCV between somites 9 and 16 on both sides of the embryo. The number of Prox1-positive endothelial cells between somites 8 and 16 was counted in embryos derived from at least three clutches of embryos. For rescue experiments, Prox1- and Myc-positive cells between somites 4 and 16 were scored in angiogenic sprouts and the PCV. All embryos were subjected to genotyping following phenotypic analysis. Student's *t*-test was used to calculate significance for quantification of cell numbers. Fisher's exact test was used to determine significance when comparing the degree of penetrance of observed phenotypes.

Acknowledgements

We are grateful to Arndt Siekmann for providing the *cdh5:gal4ff* line. We thank Phil Crosier and John Astin for the kind gift of the *lyve1b:dsRed* transgenic line. We thank members of the Lawson Lab for technical and intellectual input and the UMass Med Aquatics staff for excellent fish care.

Competing interests

The authors declare no competing or financial interests.

Author contributions

M.S. designed and performed experiments for all aspects of this work and contributed to editing of the manuscript. I.M. and T.J.B. contributed to identification and maintenance of all zebrafish lines described in this study. J.A.V. generated and validated initial Fv2E-Flt4 constructs. F.O.K. generated the *flt4*^{um131} allele. L.J.Z. performed statistical analyses. N.D.L. designed experiments and wrote the manuscript.

Funding

This work was supported by grants from the National Heart, Lung, and Blood Institute (NHLBI) [R01HL122599 and R01HL079266 to N.D.L.]; by the Uehara Memorial Foundation (M.S.); and by the Japan Society for the Promotion of Science (JSPS). Deposited in PMC for release after 12 months.

Supplementary information

Supplementary information available online at
http://dev.biologists.org/lookup/doi/10.1242/dev.137901.supplemental

References

Alitalo, K. (2011). The lymphatic vasculature in disease. *Nat. Med.* **17**, 1371-1380.

Astin, J. W., Haggerty, M. J. L., Okuda, K. S., Le Guen, L., Misa, J. P., Tromp, A., Hogan, B. M., Crosier, K. E. and Crosier, P. S. (2014). Vegfd can compensate for loss of Vegfc in zebrafish facial lymphatic sprouting. *Development* **141**, 2680-2690.

Bahram, F. and Claesson-Welsh, L. (2010). VEGF-mediated signal transduction in lymphatic endothelial cells. *Pathophysiology* **17**, 253-261.

Blackburn, P. R., Campbell, J. M., Clark, K. J. and Ekker, S. C. (2013). The CRISPR system–keeping zebrafish gene targeting fresh. *Zebrafish* **10**, 116-118.

Boscolo, E., Coma, S., Luks, V. L., Greene, A. K., Klagsbrun, M., Warman, M. L. and Bischoff, J. (2015). AKT hyper-phosphorylation associated with PI3K mutations in lymphatic endothelial cells from a patient with lymphatic malformation. *Angiogenesis* **18**, 151-162.

Bussmann, J., Wolfe, S. A. and Siekmann, A. F. (2011). Arterial-venous network formation during brain vascularization involves hemodynamic regulation of chemokine signaling. *Development* **138**, 1717-1726.

Choi, J., Dong, L., Ahn, J., Dao, D., Hammerschmidt, M. and Chen, J.-N. (2007). FoxH1 negatively modulates flk1 gene expression and vascular formation in zebrafish. *Dev. Biol.* **304**, 735-744.

Christian, M., Cermak, T., Doyle, E. L., Schmidt, C., Zhang, F., Hummel, A., Bogdanove, A. J. and Voytas, D. F. (2010). Targeting DNA double-strand breaks with TAL effector nucleases. *Genetics* **186**, 757-761.

Covassin, L. D., Villefranc, J. A., Kacergis, M. C., Weinstein, B. M. and Lawson, N. D. (2006). Distinct genetic interactions between multiple Vegf receptors are required for development of different blood vessel types in zebrafish. *Proc. Natl. Acad. Sci. USA* **103**, 6554-6559.

Covassin, L. D., Siekmann, A. F., Kacergis, M. C., Laver, E., Moore, J. C., Villefranc, J. A., Weinstein, B. M. and Lawson, N. D. (2009). A genetic screen for vascular mutants in zebrafish reveals dynamic roles for Vegf/Plcg1 signaling during artery development. *Dev. Biol.* **329**, 212-226.

Deng, Y., Atri, D., Eichmann, A. and Simons, M. (2013). Endothelial ERK signaling controls lymphatic fate specification. *J. Clin. Invest.* **123**, 1202-1215.

Gordon, K., Schulte, D., Brice, G., Simpson, M. A., Roukens, M. G., van Impel, A., Connell, F., Kalidas, K., Jeffery, S., Mortimer, P. S. et al. (2013). Mutation in vascular endothelial growth factor-C, a ligand for vascular endothelial growth factor receptor-3, is associated with autosomal dominant milroy-like primary lymphedema. *Circ. Res.* **112**, 956-960.

Hogan, B. M., Bos, F. L., Bussmann, J., Witte, M., Chi, N. C., Duckers, H. J. and Schulte-Merker, S. (2009a). Ccbe1 is required for embryonic lymphangiogenesis and venous sprouting. *Nat. Genet.* **41**, 396-398.

Hogan, B. M., Herpers, R., Witte, M., Helotera, H., Alitalo, K., Duckers, H. J. and Schulte-Merker, S. (2009b). Vegfc/Flt4 signalling is suppressed by Dll4 in developing zebrafish intersegmental arteries. *Development* **136**, 4001-4009.

Isogai, S., Lawson, N. D., Torrealday, S., Horiguchi, M. and Weinstein, B. M. (2003). Angiogenic network formation in the developing vertebrate trunk. *Development* **130**, 5281-5290.

Kaipainen, A., Korhonen, J., Mustonen, T., van Hinsbergh, V. W., Fang, G. H., Dumont, D., Breitman, M. and Alitalo, K. (1995). Expression of the fms-like tyrosine kinase 4 gene becomes restricted to lymphatic endothelium during development. *Proc. Natl. Acad. Sci. USA* **92**, 3566-3570.

Karkkainen, M. J., Ferrell, R. E., Lawrence, E. C., Kimak, M. A., Levinson, K. L., McTigue, M. A., Alitalo, K. and Finegold, D. N. (2000). Missense mutations interfere with VEGFR-3 signalling in primary lymphoedema. *Nat. Genet.* **25**, 153-159.

Karkkainen, M. J., Haiko, P., Sainio, K., Partanen, J., Taipale, J., Petrova, T. V., Jeltsch, M., Jackson, D. G., Talikka, M., Rauvala, H. et al. (2004). Vascular endothelial growth factor C is required for sprouting of the first lymphatic vessels from embryonic veins. *Nat. Immunol.* **5**, 74-80.

Kim, J.-D. and Jin, S.-W. (2014). A tale of two models: mouse and zebrafish as complementary models for lymphatic studies. *Mol. Cells* **37**, 503-510.

Development (2016) 143, 3785-3795 doi:10.1242/dev.137901

Klinghoffer, R. A., Hamilton, T. G., Hoch, R. and Soriano, P. (2002). An allelic series at the PDGFalphaR locus indicates unequal contributions of distinct signaling pathways during development. *Dev. Cell* **2**, 103-113.

Koch, S., Tugues, S., Li, X., Gualandi, L. and Claesson-Welsh, L. (2011). Signal transduction by vascular endothelial growth factor receptors. *Biochem. J.* **437**, 169-183.

Koga, A., Cheah, F. S. H., Hamaguchi, S., Yeo, G. H. and Chong, S. S. (2008). Germline transgenesis of zebrafish using the medaka Tol1 transposon system. *Dev. Dyn.* **237**, 2466-2474.

Kok, F. O., Gupta, A., Lawson, N. D. and Wolfe, S. A. (2014). Construction and application of site-specific artificial nucleases for targeted gene editing. *Methods Mol. Biol.* **1101**, 267-303.

Kok, F. O., Shin, M., Ni, C.-W., Gupta, A., Grosse, A. S., van Impel, A., Kirchmaier, B. C., Peterson-Maduro, J., Kourkoulis, G., Male, I. et al. (2015). Reverse genetic screening reveals poor correlation between morpholino-induced and mutant phenotypes in zebrafish. *Dev. Cell* **32**, 97-108.

Koltowska, K., Lagendijk, A. K., Pichol-Thievend, C., Fischer, J. C., Francois, M., Ober, E. A., Yap, A. S. and Hogan, B. M. (2015). Vegfc regulates bipotential precursor division and Prox1 expression to promote lymphatic identity in zebrafish. *Cell Rep.* **13**, 1828-1841.

Kuchler, A. M., Gjini, E., Peterson-Maduro, J., Cancilla, B., Wolburg, H. and Schulte-Merker, S. (2006). Development of the zebrafish lymphatic system requires VEGFC signaling. *Curr. Biol.* **16**, 1244-1248.

Kwan, K. M., Fujimoto, E., Grabher, C., Mangum, B. D., Hardy, M. E., Campbell, D. S., Parant, J. M., Yost, H. J., Kanki, J. P. and Chien, C.-B. (2007). The Tol2kit: a multisite gateway-based construction kit for Tol2 transposon transgenesis constructs. *Dev. Dyn.* **236**, 3088-3099.

Lapinski, P. E., Kwon, S., Lubeck, B. A., Wilkinson, J. E., Srinivasan, R. S., Sevick-Muraca, E. and King, P. D. (2012). RASA1 maintains the lymphatic vasculature in a quiescent functional state in mice. *J. Clin. Invest.* **122**, 733-747.

Lawson, N. D. and Weinstein, B. M. (2002). In vivo imaging of embryonic vascular development using transgenic zebrafish. *Dev. Biol.* **248**, 307-318.

Lawson, N. D., Mugford, J. W., Diamond, B. A. and Weinstein, B. M. (2003). phospholipase C gamma-1 is required downstream of vascular endothelial growth factor during arterial development. *Genes Dev.* **17**, 1346-1351.

Makinen, T., Veikkola, T., Mustjoki, S., Karpanen, T., Catimel, B., Nice, E. C., Wise, L., Mercer, A., Kowalski, H., Kerjaschki, D. et al. (2001). Isolated lymphatic endothelial cells transduce growth, survival and migratory signals via the VEGF-C/D receptor VEGFR-3. *EMBO J.* **20**, 4762-4773.

Meng, X., Noyes, M. B., Zhu, L. J., Lawson, N. D. and Wolfe, S. A. (2008). Targeted gene inactivation in zebrafish using engineered zinc-finger nucleases. *Nat. Biotechnol.* **26**, 695-701.

Mouta-Bellum, C., Kirov, A., Miceli-Libby, L., Mancini, M. L., Petrova, T. V., Liaw, L., Prudovsky, I., Thorpe, P. E., Miura, N., Cantley, L. C. et al. (2009). Organ-specific lymphangiectasia, arrested lymphatic sprouting, and maturation defects resulting from gene-targeting of the PI3K regulatory isoforms p85alpha, p55alpha, and p50alpha. *Dev. Dyn.* **238**, 2670-2679.

Mulligan, T. S. and Weinstein, B. M. (2014). Emerging from the PAC: studying zebrafish lymphatic development. *Microvasc. Res.* **96**, 23-30.

Nicenboim, J., Malkinson, G., Lupo, T., Asaf, L., Sela, Y., Mayseless, O., Gibbs-Bar, L., Senderovich, N., Hashimshony, T., Shin, M. et al. (2015). Lymphatic vessels arise from specialized angioblasts within a venous niche. *Nature* **522**, 56-61.

Okuda, K. S., Astin, J. W., Misa, J. P., Flores, M. V., Crosier, K. E. and Crosier, P. S. (2012). lyve1 expression reveals novel lymphatic vessels and new mechanisms for lymphatic vessel development in zebrafish. *Development* **139**, 2381-2391.

Pajusola, K., Aprelikova, O., Pelicci, G., Weich, H., Claesson-Welsh, L. and Alitalo, K. (1994). Signalling properties of FLT4, a proteolytically processed receptor tyrosine kinase related to two VEGF receptors. *Oncogene* **9**, 3545-3555.

Sakurai, Y., Ohgimoto, K., Kataoka, Y., Yoshida, N. and Shibuya, M. (2005). Essential role of Flk-1 (VEGF receptor 2) tyrosine residue 1173 in vasculogenesis in mice. *Proc. Natl. Acad. Sci. USA* **102**, 1076-1081.

Salameh, A., Galvagni, F., Bardelli, M., Bussolino, F. and Oliviero, S. (2005). Direct recruitment of CRK and GRB2 to VEGFR-3 induces proliferation, migration, and survival of endothelial cells through the activation of ERK, AKT, and JNK pathways. *Blood* **106**, 3423-3431.

Schramek, H., Feifel, E., Healy, E. and Pollack, V. (1997). Constitutively active mutant of the mitogen-activated protein kinase kinase MEK1 induces epithelial dedifferentiation and growth inhibition in madin-darby canine kidney-C7 cells. *J. Biol. Chem.* **272**, 11426-11433.

Siekmann, A. F. and Lawson, N. D. (2007). Notch signalling limits angiogenic cell behaviour in developing zebrafish arteries. *Nature* **445**, 781-784.

Siekmann, A. F., Standley, C., Fogarty, K. E., Wolfe, S. A. and Lawson, N. D. (2009). Chemokine signaling guides regional patterning of the first embryonic artery. *Genes Dev.* **23**, 2272-2277.

Takahashi, T., Yamaguchi, S., Chida, K. and Shibuya, M. (2001). A single autophosphorylation site on KDR/Flk-1 is essential for VEGF-A-dependent activation of PLC-gamma and DNA synthesis in vascular endothelial cells. *EMBO J.* **20**, 2768-2778.

Tallquist, M. D., Klinghoffer, R. A., Heuchel, R., Mueting-Nelsen, P. F., Corrin, P. D., Heldin, C.-H., Johnson, R. J. and Soriano, P. (2000). Retention of PDGFR-beta function in mice in the absence of phosphatidylinositol 3′-kinase and phospholipase Cgamma signaling pathways. *Genes Dev.* **14**, 3179-3190.

Tammela, T., Zarkada, G., Wallgard, E., Murtomaki, A., Suchting, S., Wirzenius, M., Waltari, M., Hellstrom, M., Schomber, T., Peltonen, R. et al. (2008). Blocking VEGFR-3 suppresses angiogenic sprouting and vascular network formation. *Nature* **454**, 656-660.

Taniguchi, K., Kohno, R.-I., Ayada, T., Kato, R., Ichiyama, K., Morisada, T., Oike, Y., Yonemitsu, Y., Maehara, Y. and Yoshimura, A. (2007). Spreds are essential for embryonic lymphangiogenesis by regulating vascular endothelial growth factor receptor 3 signaling. *Mol. Cell. Biol.* **27**, 4541-4550.

Thompson, M. A., Ransom, D. G., Pratt, S. J., MacLennan, H., Kieran, M. W., Detrich, H. W., III, Vail, B., Huber, T. L., Paw, B., Brownlie, A. J. et al. (1998). The cloche and spadetail genes differentially affect hematopoiesis and vasculogenesis. *Dev. Biol.* **197**, 248-269.

Traver, D., Paw, B. H., Poss, K. D., Penberthy, W. T., Lin, S. and Zon, L. I. (2003). Transplantation and in vivo imaging of multilineage engraftment in zebrafish bloodless mutants. *Nat. Immunol.* **4**, 1238-1246.

Tvorogov, D., Anisimov, A., Zheng, W., Leppanen, V.-M., Tammela, T., Laurinavicius, S., Holnthoner, W., Helotera, H., Holopainen, T., Jeltsch, M. et al. (2010). Effective suppression of vascular network formation by combination of antibodies blocking VEGFR ligand binding and receptor dimerization. *Cancer Cell* **18**, 630-640.

Villefranc, J. A., Amigo, J. and Lawson, N. D. (2007). Gateway compatible vectors for analysis of gene function in the zebrafish. *Dev. Dyn.* **236**, 3077-3087.

Villefranc, J. A., Nicoli, S., Bentley, K., Jeltsch, M., Zarkada, G., Moore, J. C., Gerhardt, H., Alitalo, K. and Lawson, N. D. (2013). A truncation allele in vascular endothelial growth factor c reveals distinct modes of signaling during lymphatic and vascular development. *Development* **140**, 1497-1506.

Wang, Y., Nakayama, M., Pitulescu, M. E., Schmidt, T. S., Bochenek, M. L., Sakakibara, A., Adams, S., Davy, A., Deutsch, U., Luthi, U. et al. (2010). Ephrin-B2 controls VEGF-induced angiogenesis and lymphangiogenesis. *Nature* **465**, 483-486.

Yaniv, K., Isogai, S., Castranova, D., Dye, L., Hitomi, J. and Weinstein, B. M. (2006). Live imaging of lymphatic development in the zebrafish. *Nat. Med.* **12**, 711-716.